The Journal of Immunology

Identification of *Drosophila* Zfh2 as a Mediator of Hypercapnic Immune Regulation by a Genome-Wide RNA Interference Screen

Iiro Taneli Helenius, Ryan J. Haake, Yong-Jae Kwon, Jennifer A. Hu, Thomas Krupinski, S. Marina Casalino-Matsuda, Peter H. S. Sporn, Jacob I. Sznajder and Greg J. Beitel

J Immunol 2016; 196:655-667; Prepublished online 7 December 2015;
doi: 10.4049/jimmunol.1501708
http://www.jimmunol.org/content/196/2/655

The Journal of Immunology is published twice each month by
The American Association of Immunologists, Inc.,
9650 Rockville Pike, Bethesda, MD 20814-3994.

Print ISSN: 0022-1767 Online ISSN: 1550-6606.

Identification of *Drosophila* Zfh2 as a Mediator of Hypercapnic Immune Regulation by a Genome-Wide RNA Interference Screen

Iiro Taneli Helenius,*,†,1,2 Ryan J. Haake,*,1 Yong-Jae Kwon,* Jennifer A. Hu,* Thomas Krupinski,* S. Marina Casalino-Matsuda,† Peter H. S. Sporn,†,‡ Jacob I. Sznajder,† and Greg J. Beitel*

Hypercapnia, elevated partial pressure of CO_2 in blood and tissue, develops in many patients with chronic severe obstructive pulmonary disease and other advanced lung disorders. Patients with advanced disease frequently develop bacterial lung infections, and hypercapnia is a risk factor for mortality in such individuals. We previously demonstrated that hypercapnia suppresses induction of NF-κB–regulated innate immune response genes required for host defense in human, mouse, and *Drosophila* cells, and it increases mortality from bacterial infections in both mice and *Drosophila*. However, the molecular mediators of hypercapnic immune suppression are undefined. In this study, we report a genome-wide RNA interference screen in *Drosophila* S2* cells stimulated with bacterial peptidoglycan. The screen identified 16 genes with human orthologs whose knockdown reduced hypercapnic suppression of the gene encoding the antimicrobial peptide Diptericin (Dipt), but did not increase *Dipt* mRNA levels in air. In vivo tests of one of the strongest screen hits, zinc finger homeodomain 2 (Zfh2; mammalian orthologs ZFHX3/ATBF1 and ZFHX4), demonstrate that reducing *zfh2* function using a mutation or RNA interference improves survival of flies exposed to elevated CO_2 and infected with *Staphylococcus aureus*. Tissue-specific knockdown of *zfh2* in the fat body, the major immune and metabolic organ of the fly, mitigates hypercapnia-induced reductions in *Dipt* and other antimicrobial peptides and improves resistance of CO_2-exposed flies to infection. *Zfh2* mutations also partially rescue hypercapnia-induced delays in egg hatching, suggesting that Zfh2's role in mediating responses to hypercapnia extends beyond the immune system. Taken together, to our knowledge, these results identify Zfh2 as the first in vivo mediator of hypercapnic immune suppression. *The Journal of Immunology*, 2016, 196: 655–667.

Hypercapnia, elevation of blood and tissue levels of CO_2, develops in many patients with severe chronic obstructive pulmonary disease (COPD), currently the third leading cause of death in the United States (1), and other advanced lung diseases. Hypercapnia has long been recognized as a risk factor for mortality in patients with acute exacerbations of COPD (2–6), and recently it was shown that use of nocturnal ventilatory support to decrease CO_2 levels improved survival of hypercapnic patients with COPD (7). Acute exacerbations of COPD, which are linked to mortality, are most commonly triggered by bacterial or viral respiratory infections (8–10). Hypercapnia is also a risk factor for mortality in patients hospitalized with community-acquired pneumonia (11, 12), children with adenoviral lung infections (13), and cystic fibrosis patients awaiting lung transplantation (14). These observations suggest that hypercapnia may contribute to poor clinical outcomes by increasing susceptibility to pulmonary infections.

Consistent with this hypothesis, we and others have shown that hypercapnia inhibits expression of IL-6, TNF, and other cytokines important for host defense (15–17). Cummins and colleagues (18, 19) have shown that elevated CO_2 inhibits activation of the canonical NF-κB pathway that drives expression of many host defense genes while promoting activation of the noncanonical NF-κB component RelB (18, 19), whose function is largely anti-inflammatory and immunosuppressive. We also showed that hypercapnia suppresses phagocytosis, generation of reactive oxygen

*Department of Molecular Biosciences, Northwestern University, Evanston, IL 60208; †Division of Pulmonary and Critical Care Medicine, Feinberg School of Medicine, Northwestern University, Chicago, IL 60611; and ‡Jesse Brown Veterans Affairs Medical Center, Chicago, IL 60612

[1]I.T.H. and R.J.H. contributed equally to this work.

[2]Current address: Cardiovascular Research Center, Massachusetts General Hospital, Charlestown, MA.

ORCIDs: 0000-0002-7566-4560 (S.M.C.-M.); 0000-0002-2089-4764 (J.I.S.); 0000-0003-4413-6324 (G.J.B.).

Received for publication July 29, 2015. Accepted for publication November 2, 2015.

This work was supported by National Institutes of Health/National Heart, Lung, and Blood Institute Grants R01 HL107629 (to G.J.B. and P.H.S.S.) and R01 HL085534 and R01 HL071643 (to J.I.S.), as well as by grants from the *Drosophila* RNAi Screening Center (National Institute of General Medical Sciences Grant R01 GM067761), the RNAi Project at Harvard Medical School (National Institutes Health/National Institute of General Medical Sciences Grant R01 GM084947), and the Bloomington *Drosophila* Stock Center (National Institutes of Health Grant P40 OD018537), the Northwestern University Robert H. Lurie Comprehensive Cancer Center to the Northwestern University High Throughput Analysis Laboratory, and by American Heart Association Grant-in-Aid Award 0855686G (to G.J.B.) and Predoctoral Fellowship 0715562Z (to I.T.H.)

I.T.H., R.J.H., P.H.S.S., J.I.S., and G.J.B. designed research; I.T.H., R.J.H., Y.-J.K., J.A.H., T.K., and S.M.C.-M. performed research; all authors contributed to data analysis; and I.T.H., R.J.H., P.H.S.S., and G.J.B. wrote the paper.

Address correspondence and reprint requests to Dr. Greg J. Beitel, Northwestern University, Hogan Hall, 2205 Tech Drive, Room 2-100, Evanston, IL 60208. E-mail address: beitel@northwestern.edu

The online version of this article contains supplemental material.

Abbreviations used in this article: AMP, antimicrobial peptide; Att, Attacin; Cec, Cecropin; COPD, chronic obstructive pulmonary disease; Dipt, Diptericin; *Dipt-luc*, firefly *Diptericin-luciferase*; Drs, Drosomycin; DRSC, *Drosophila* RNAi Screening Center; Imd, immune deficiency; Mtk, Metchnikowin; PGN, peptidoglycan; *polIII-luc*, *Renilla polIII-luciferase*; qPCR, quantitative PCR; RNAi, RNA interference; Zfh2, zinc finger homeodomain 2.

www.jimmunol.org/cgi/doi/10.4049/jimmunol.1501708

species, and autophagy (15–17), all key phagocyte antimicrobial functions. Furthermore, we showed that hypercapnia reduces bacterial clearance and increases mortality in a mouse model of *Pseudomonas* pneumonia (16). Despite these observations, the molecular mechanisms by which elevated CO_2 levels are sensed and transduced in immune cells are not yet understood.

One way that elevated CO_2 might influence immune responses is by reducing extracellular and/or intracellular pH; indeed, there is evidence that acidosis may decrease the function of various immune cells (20). However, in our in vitro studies, suppression of cytokine gene expression, phagocytosis, and autophagy by elevated CO_2 levels was independent of acidosis (15–17). Furthermore, hypercapnia increased the mortality of bacterial pneumonia in mice with acute and chronic hypercapnia to the same degree, despite more severe acidosis in animals with acute hypercapnia compared with chronic hypercapnia (due to renal compensation in the latter group) (16). Taken together, these results suggest that molecular CO_2 has immune suppressive effects that are experimentally and physiologically distinguishable from the effects of acidosis.

To investigate the molecular mechanisms of hypercapnic immune suppression, we studied *Drosophila* as a tractable molecular genetic model system for nonneuronal responses to elevated CO_2 (21). The response to hypercapnia in *Drosophila* and mammals has multiple parallels (15, 16): elevated CO_2 levels suppress production of *Drosophila* immune response genes in vivo and in vitro at the transcriptional level via a mechanism that is downstream of NF-κB proteolytic activation. As in mammalian macrophages, downregulation of immune response genes was independent of pH. Hypercapnia also significantly decreases resistance of adult flies to bacterial infections. The similarities of hypercapnic immune suppression in flies and mammals, in combination with evidence that a conserved JNK pathway controls Na,K-ATPase endocytosis during hypercapnia (22), suggest that elevated CO_2 acts via specific evolutionarily conserved pathways to downregulate host defenses.

In this study, we describe the results of a genome-wide RNA interference (RNAi) screen in *Drosophila* S2* cells to identify mediators of CO_2-induced immune suppression. The screen identified >16 genes with human orthologs whose knockdown attenuates hypercapnic suppression of the antimicrobial peptide (AMP) gene in peptidoglycan (PGN)-stimulated S2* cells. In vivo characterization of one of these genes, the transcription factor zinc finger homeodomain 2 (*zfh2*; mammalian orthologs ZFHX3/ATBF1 and ZFHX4), shows that reducing Zfh2 levels in the major immune organ of the fly, the fat body, improves resistance and survival to *Staphylococcus aureus* infection during hypercapnia. To our knowledge, this is the first description of a component of CO_2 response pathways that mediate the in vivo effects of hypercapnia on immune responses.

Materials and Methods

CO_2 treatment for cell lines and flies

Exposures to air (normocapnia: 0.039% CO_2, 21% O_2, 78% N_2) and elevated CO_2 were carried out in BioSpherix C-Chambers fitted with ProCO$_2$ regulators and CO_2 and O_2 sensors. CO_2 (100%) was injected into the chambers to raise the ambient CO_2 levels to either 5% CO_2 (mild hypercapnia: 5.0% CO_2, 20% O_2, 74% N_2) or 13% CO_2 (hypercapnia: 13.0% CO_2, 18% O_2, 68% N_2). For fly experiments, humidity was maintained at ~60% using Drierite.

RNAi screening

Pilot screening was performed at Northwestern University's High Throughput Analysis Laboratory using the S2* *Diptericin-luciferase* (*Dipt-luc*) cell line (gift from N. Silverman). The *Dipt-luc* reporter consists of 2.2 kb of the *Dipt* promoter (23) driving firefly luciferase in the pGL3 vector (Promega) (24). A *Renilla luciferase-Pol III* (*polIII-luc*) reporter, in which a fragment of the promoter for the RNA polymerase 128 subunit drives *Renilla* luciferase (25) (gift of the *Drosophila* RNAi Screening Center [DRSC], Harvard Medical School, Boston, MA), was transfected into the *Dipt-luc* cell line using Effectene (Qiagen). Selected PCR amplicons were obtained from the DRSC and in vitro transcribed using the T7 MEGAscript kit (no. AMB1334, Applied Biosystems) into dsRNAs using DRSC protocols (26). Cells were maintained in 1 mg/ml G418 and 200 μg/ml hygromycin in Schneider's insect medium (Sigma-Aldrich) containing 10% FBS. All liquid handling was performed using a Matrix WellMate dispenser (Thermo Scientific). Five hundred cells per well in 384-well plates were bathed with preplated dsRNAs (~1–5 μg total dsRNA) for 3 d prior to CO_2 exposure to ensure effective gene knockdown. Nineteen hours prior to CO_2 exposure, cells were primed with 1 μM 20-hydroxyecdysone (Sigma-Aldrich) to improve immune responsiveness. Cells were exposed to 13% CO_2 for 10 h in media neutralized with 25 mM NaOH to maintain pH at 7.1 as previously described (21). Five hours after the start of CO_2 exposure, cells were challenged with 100 ng/ml *E. coli* PGN (*E. coli* 0111:B4, InvivoGen) to induce *Dipt*. Firefly and *Renilla* luminescence was measured sequentially using Dual-Glo luciferase reagent (Promega) with an Analyst GT plate reader (Molecular Devices). Data were analyzed using DRSC software and Microsoft Excel. Primary RNAi screening was carried out in duplicate in 13% CO_2; these experiments were performed on-site at the DRSC. The raw data from the primary screen are available from the DRSC under project ID 128 at http://www.flyrnai.org/cgi-bin/DRSC_screen_csv.pl?project_id=128, and the normalized and formatted data are shown in Supplemental Table II.

dsRNAs of interest were identified based on their *Z*-score, which represents the number of standard deviations the signal from one well on a plate is above or below the plate mean. *Z*-scores were calculated by normalizing the *Dipt-luc* signal from each well to the *polIII-luc* signal from the same well, calculating the average *Dipt-luc/polIII-luc* ratio on a plate, and determining the deviation of each well from the plate average.

Secondary screening was performed in 13% CO_2 in duplicate wells of duplicate 96-well plates filled using multichannel pipettes. A *Z*-score was calculated for each dsRNA by averaging the *Z*-scores for the dsRNAs on each of the two independent plates. Tertiary screening was performed as per secondary screening, except that duplicate plates with two dsRNAs on a plate were each screened in air and 13% CO_2.

Fly stocks and maintenance

Drosophila stocks were kept on cornmeal food at room temperature or at 25˚C. Stocks were obtained from the Bloomington Stock Center unless otherwise specified. $zfh2^{MS209}$ (27), $zfh2^{2\text{-}M390.R}$ (28), and $zfh2^{1\text{-}M707.R}$ (28) were backcrossed five times to w^{1118} prior to infection experiments ($zfh2^{1\text{-}M707.R}$ and $zfh2^{2\text{-}M390.R}$ were provided by S. Elgin). The w^{1118} stock used for backcrossing was used as a control for *zfh2* mutant experiments. For RNAi knockdown of *zfh2*, *CG-GAL4* (29) and *C754-GAL4* (30) were used to express *UAS-*$zfh2^{13305}$ (31) in the fat body. Control crosses for knockdown experiments used the w^{1118} isogenic strain V60000 from which *UAS-*$zfh2^{13305}$ was derived.

Western blotting

Western blotting was performed using ~10^6 S2* cells per sample, 20 fly heads, 20 dissected male abdominal fat bodies, or 20 carcasses after head and fat body removal. Fat bodies were dissected using the protocol of Krupp and Levine (32). For *S. aureus* challenge, samples were collected 4 h postinfection. Samples were run on 4% acrylamide gels and transferred to nitrocellulose membrane by electroblotting at 100 V for 80 min. Membranes were blocked with 5% skim milk in TBST (20 mM Tris-Cl [pH 7.5], 150 mM NaCl, 0.1% Tween 20), incubated overnight with 1:500 rat anti-Zfh2 sera no. 205 (33), then 45 min with 1:10,000 goat anti-rat IgG-HRP (sc-2065, Santa Cruz Biotechnology). Actin (as a loading control) was detected using 1:200 mouse mAb JLA20 (Developmental Studies Hybridoma Bank) and 1:10,000 goat anti-mouse IgG-HRP (170-6516, Bio-Rad Laboratories). Amersham ECL Prime Western blotting detection reagent (RPN2232, GE Healthcare Life Sciences) was used for detection, and chemiluminescence of bands was quantitated with the Odyssey Fc imaging system (LI-COR Biosciences).

Fly infection assays

Fly infection and mortality tests were performed on adult male flies as described in Helenius et al. (21). Bacterial load assays for Fig. 4E were performed as described in Helenius et al. (21), and for Fig. 4G were determined 16–18 h postinfection by washing single flies with 75% ethanol, rinsing with Luria–Bertani media, and then homogenizing in 200 μl fresh

Luria–Bertani media. Homogenates were centrifuged on a bench-top centrifuge for 3 min at 2000 rpm, and 100 μl bacterial supernatant was transferred to 1.9 ml fresh Luria–Bertani media and then shaken at 37°C for 8 h, at which time OD_{600} was determined.

Ex vivo fat body culture

For each experiment, three dissected fat bodies (see above) were placed in 1 ml S2* media (described above) and cultured in one well of a 24-well plate for 24 h in media equilibrated with air or 13% CO_2. PGN treatment and media conditions were as for S2* cell induction (21). Total RNA was obtained from fat bodies using TRIzol LS (no. 10296-028, Life Technologies). Quantitative PCR (qPCR) was performed per the manufacturer's protocol using the iScript cDNA synthesis kit (no. 170-8891, Bio-Rad Laboratories), the iTaq Universal SYBR Green Supermix (no. 172-5124, Bio-Rad Laboratories), and the *Dipt* primers 5′-ACCGCAGTACCCACTCAATC-3′ and 5′-ACTTTCCAGCTCGGTTCTGA-3′. Primers for Attacin (*Att*), Cecropin (*Cec*), Drosomycin (*Drs*), and Metchnikowin (*Mtk*) were as previously described (21).

Statistical analysis

Data are presented as means ± SEM. GraphPad Prism (version 5.04) and SigmaPlot (version 11.0) were used for statistical analysis. Differences between two groups were assessed using a Student *t* test. Differences between multiple groups were assessed by ANOVA and the Tukey range test. For comparison of bacterial CFU data, the $\log_{10}$ values were used in the analysis. For mortality experiments, the Gehan–Breslow–Wilcoxon test was used. Significance was accepted at $p < 0.05$.

Results

Dipt-luc *is a CO_2-responsive reporter of innate immune responses*

We had previously established *Drosophila* S2* cells as a model for investigating hypercapnic immune suppression by showing that *E. coli* PGN-stimulated induction of the mRNA for the antimicrobial peptide Dipt was suppressed by hypercapnia in a concentration-dependent manner, without any cytotoxicity (21). In principle, this suppression could be the basis for a genome-wide screen to identify genes that mediate CO_2-induced immune suppression. However, the previously used qPCR-based approach was poorly suited to high-throughput assays. We therefore tested whether the firefly *Dipt-luc* construct containing 2.2 kb of the *Dipt* promoter (24) would show the same CO_2-induced suppression as the endogenous *Dipt* gene. We also tested whether expression of a *Renilla luciferase* driven by the promoter for the RNA polymerase III 128 subunit (*polIII-luc*) (25) was independent of CO_2 levels, which would enable it to be used as an internal control to account for treatment effects on cell growth and viability. In S2* cells stably transfected with the *Dipt-luc* and *polIII-luc* constructs, PGN-induced expression of the *Dipt-luc* reporter was suppressed ~5-fold in 13% CO_2 compared with expression in air, whereas *polIII-luc* reporter expression was unaffected by elevated CO_2 (Fig. 1A). Further testing established that the signal from the *Dipt-luc* construct also closely paralleled endogenous *Dipt* mRNA levels in mild hypercapnia (5% CO_2 for a total of 10 h), sustained hypercapnia (13% CO_2 for a total of 24 h), and during an 8-h time course following induction with PGN in air and 13% CO_2 (Fig. 1B, 1C). Critically, signals from both *Dipt-luc* and *polIII-luc* were robustly detected from cells in 384-well plates. Thus, the *Dipt-luc*/*polIII-luc* combination appeared suitable for high-throughput screening.

Hypercapnic immune suppression is not mediated by carbonic anhydrases or dJNK

Prior to performing a genome-wide RNAi screen, we conducted a pilot screen using S2* cells expressing *Dipt-luc* and *polIII-luc* at the Northwestern University's High Throughput Analysis Laboratory. We tested a panel of dsRNAs targeting candidate genes that had previously been shown either to regulate AMP expression, to act in CO_2-responsive pathways in other systems, or to interact biochemically with molecular CO_2 and therefore plausibly mediate hypercapnic immune suppression (Supplemental Table I). dsRNAs targeting the firefly and *Renilla* luciferases were used to confirm efficiency of RNAi knockdown. Knockdown of components of the immune deficiency (Imd) pathway that regulates AMP expression either reduced (e.g., *imd*, *rel*) or increased (e.g., *caspar*) *Dipt-luc* expression as expected based on their known roles in regulation of *Dipt* expression, thus confirming the integrity of the assay (Supplemental Table I). A dsRNA (DRSC amplicon DRSC00843) targeting the gene *u-shaped*, a known regulator of AMP expression (34), typically upregulated expression of the *Dipt-luc* reporter in both air and elevated CO_2, and was used as a positive control in subsequent experiments (e.g., Fig. 1D).

One of the most interesting a priori candidate CO_2 regulators was JNK, an evolutionarily conserved modulator of the immune system that we had previously shown to be required for Na,K-ATPase endocytosis in response to elevated CO_2 levels in both *Drosophila* S2 and mammalian lung epithelial cells (22). However, RNAi-mediated knockdown of *Drosophila* JNK (*basket*) did not mitigate hypercapnic suppression of *Dipt-luc* in S2* cells (Fig. 1D). Other candidates of particular interest were CO_2-binding carbonic anhydrases. Flies have two conventional carbonic anhydrases, *CAH1* and *CAH2*, and an ortholog of the noncanonical nuclear carbonic anhydrase nonO/p54, called *nonA* (35). However, RNAi knockdown of *nonA* alone or in combination with *CAH1* and *CAH2* did not abrogate the suppression of the *Dipt-luc* reporter by hypercapnia (Fig. 1D). Similar negative results were obtained with the other 34 candidate genes tested, including components of NO and hypoxia response pathways, components of the Imd pathway, and *Gr63a/Gr21a* that comprise the fly neuronal CO_2 sensor (Supplemental Table I). That none of the dsRNAs targeting candidate genes caused significant differential effects in air versus elevated CO_2 suggests that hypercapnic immune suppression is mediated by novel mechanisms and underscores the need for discovery-based approaches to identify components of CO_2 response pathways.

A genome-wide RNAi screen for components of CO_2 response pathways

We next performed a genome-wide screen at the Harvard DRSC, using the DRSC 2.0 library that covered 13,900 of the ~14,000 annotated *Drosophila* genes (36), at an average of between one and two dsRNAs per gene. The dsRNA library was tested in duplicate in 384-well plates in 13% CO_2 in media adjusted to pH 7.0 (see Fig. 1E for screen workflow; additional details are in *Materials and Methods*). The primary genome-wide screen was performed only in 13% CO_2. The full results of the screen have been deposited with the Harvard DRSC and are available at http://www.flyrnai.org/screensummary. As described below, top hits from the primary screen were further tested to identify those that differentially regulated *Dipt-luc* in elevated CO_2 versus in air.

Genes of interest from the primary screen were identified as those whose knockdowns most increased *Dipt-luc* levels, after normalization with *polIII-luc*. This was quantified using the *Z*-score, which is the number of standard deviations that the normalized *Dipt-luc* level in a well treated with a given dsRNA is above or below the mean normalized *Dipt-luc* levels of all wells of the plate in which the dsRNA was arrayed (see *Materials and Methods*). The primary screen identified a total of 126 dsRNAs targeting 123 genes that had an average Z-score from duplicate plates of ≥2.5 and 496 genes that had an average *Z*-score of ≥1.5 (Supplemental Table II). The ability of the screen to identify biologically relevant regulators of immune function was confirmed

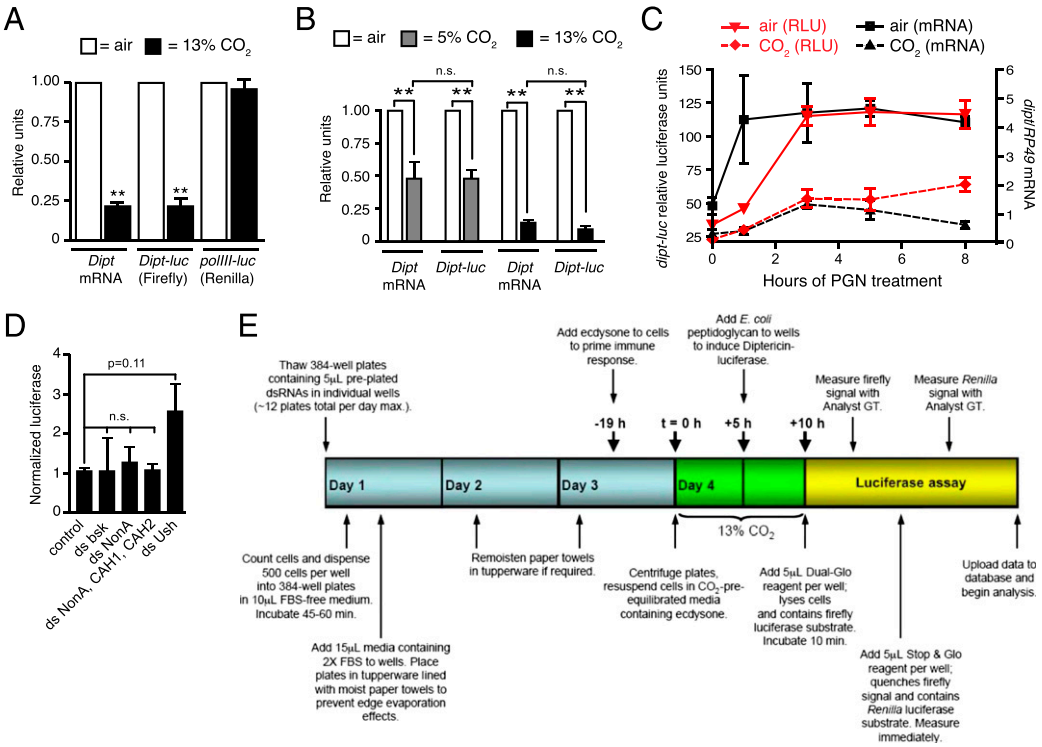

FIGURE 1. A *Dipt-luc* reporter construct enables a genome-wide screen for genes that mediate hypercapnic immune suppression. (**A**) The *Dipt-luc* reporter containing 2.2 kb of the *Dipt* promoter region driving firefly *luciferase* (23) in S2* cells closely parallels expression of the endogenous *Dipt* locus in air and in neutral hypercapnia (13% CO_2 [pH 7.1]: 5 h in 13% CO_2, then 5 h PGN in 13% CO_2). A reporter containing the promoter for the PolIII 128 subunit gene driving *Renilla luciferase* (25) is not responsive to CO_2 and was used to calculate normalized activity of the *Dipt-luc* reporter. *Dipt* mRNA levels were assessed using qPCR normalized to RP49 mRNA levels. (**B** and **C**) The *Dipt-luc* reporter closely parallels endogenous *Dipt* mRNA expression in PGN-stimulated S2* cells in (B) neutral mild hypercapnia (pH 7.1; 5 h in 5% CO_2, then 5 h PGN in 5% CO_2), in sustained neutral hypercapnia (13% CO_2, pH 7.1; 19 h in 13% CO_2, then 5 h PGN in 13% CO_2), and (C) during an 8-h time course of PGN treatment (13% CO_2, pH 7.1; 5 h pre-exposure in 13% CO_2). (**D**) dsRNAs targeting *bsk (Drosophila* JNK*)* or carbonic anhydrases do not upregulate *Dipt-luc* in elevated CO_2 (results for additional candidate genes in pilot screening are shown in Supplemental Table I). (**E**) Workflow for the genome-wide screen to identify genes that mediate hypercapnic immune suppression. For all panels, $^{**}p < 0.01$.

by the identification of several genes previously described as negative regulators of the Imd/Dipt pathway, including *falafel*, *kismet*, *cyclin D*, *enabled*, and *Ras85D* (37–39) (Supplemental Table II). The robustness of the screen was further highlighted by the identification (Z-score ≤ -1.5) of several known positive regulators of the Imd/Dipt pathway, including the PGN cell surface receptor PGRP-LC, Tak1 kinase, and the NF-κB transcription factor Relish that binds the *Dipt* promoter (Supplemental Table II). The identification of known positive and negative regulators of the Imd/Dipt pathway, as well as genes far upstream (the PGRP-LC receptor) (40–42) and immediately regulating *Dipt* expression (the Rel transcription factor that drives *Dipt* expression) (43), suggested that the screen could also identify components of a CO_2-responsive signaling pathway.

To begin assessing whether the screen identified new pathways regulating *Dipt* expression, we analyzed the genes corresponding to the dsRNAs that had a Z-score of ≥ 1.5 in the primary screen for interactions using the STRING program (44). The resulting map contained one gene known to negatively regulate the Imd pathway (Ras85D) and showed connections between genes that positively regulate protein synthesis, but did not reveal an obvious new pathway that might mediate CO_2 responses (data not shown). However, to our knowledge none of the data on the relationships between genes/proteins used by the STRING program has been generated under hypercapnia. Thus, interactions that occur specifically during conditions of elevated CO_2 would not be expected to appear in the interaction map.

Functional classification, based on gene ontology biological processes, of the genes of interest identified in the primary screen revealed that the distribution of functions of genes with a Z-score of $\geq +1.5$ or ≤ -1.5 from the screen is different from the fly genome as a whole (Supplemental Fig. 1). Furthermore, the genes whose knockdown upregulates the reporter fall into different functional groups than those whose knockdown downregulates the reporter. The group of genes that negatively regulate *Dipt* expression in hypercapnia is enriched for genes that are involved in responding to external stimuli or are involved in movement, morphogenesis, or differentiation, whereas the group of genes that positively regulate *Dipt* expression is enriched in spindle and centrosome functions (Supplemental Fig. 1). Notably, of the 126 primary hits, 51% have human orthologs based on analyses using HomoloGene (http://www.ncbi.nlm.nih.gov/homologene/) and InParanoid (45). Of those with orthologs, 25 have a Z-score of >3 (Supplemental Table II), suggesting the screen may have identified conserved genes that mediate the effects of hypercapnia on immune gene expression.

Secondary screening identifies 17 candidate mediators of CO_2-induced immune suppression

Based on strength of Z-score, presence of a human ortholog, and possible likelihood of functional significance as a CO_2 pathway signal transducer (e.g., a kinase), 192 dsRNAs (representing 192 genes) were selected for further screening (Supplemental Table II). Secondary screening was performed using the same

protocols as the primary screen, except dsRNAs were assayed in 96-well plates in quadruplicate, rather than in duplicate (see *Materials and Methods*). Of the 192 dsRNAs tested in secondary screening, 39 were found to upregulate *Dipt-luc* by at least 1 SD above the mean of all wells in at least one 96-well secondary screening plate (Supplemental Table II). Thus, secondary screening delineated 39 dsRNAs that had the strongest effects in a head-to-head comparison of the 192 dsRNAs selected from the primary screen. These 39 dsRNAs were then further tested at two different RNA concentrations in 13% CO_2 and ambient air to determine the CO_2 specificity of the upregulation of *Dipt-luc* (Fig. 2, Supplemental Table III). Candidate CO_2-response pathway components were identified as those whose knockdown preferentially upregulated *Dipt-luc* in hypercapnia but not in ambient air (Fig. 2). For 17 of the 39 candidate genes, induction of the *Dipt-luc* reporter was ≥2-fold higher in 13% CO_2 than in air at one or both of the dsRNA concentrations tested (Fig. 2, Supplemental Table III). Thus, these 17 genes, 16 of which have human orthologs, were preferentially required for hypercapnia to suppress *Dipt* induction and were designated as candidate CO_2 mediator genes.

Putative functional categories of the 17 candidate CO_2 mediators include a transcription factor (*zfh2*), chromatin-associated proteins (*zormin*, *flfl*, *rpd3*, and *trx*), regulators of signal transduction (*flfl*, *ras85D*, *rhogap15b*), a cell surface protein (*corin*), and an RNA-binding protein (*scaf6*). Interestingly, two of the candidate genes, *flfl* and *ras85D* (37), had previously been implicated in interacting with the Imd pathway, although they do not appear to act in linear order to control Imd signaling, and most proteins in the pathways with which these genes are associated did not score as hits. Gene ontology and STRING analyses of the functions and interactions of these candidate mediators did not reveal an obvious CO_2 sensor candidate or a common pathway or function among all of the genes. However, analysis of the top 17 candidate CO_2 mediators using STRING revealed known connections between *RhoGAP15B*, *Ras85D*, *Rpd3*, and *trx* (Fig. 2C). Allowing the STRING program to search for potential connections by adding 10 nodes between the top 17 hits produced an interaction network connecting *zormin* and *zfh2* to the *Rpd3* group, however, only one of these new intervening nodes, *brm*, had a *Z*-score of ≤−1 in the primary screen. These results do not support the existence of a simple single linear pathway mediating the effects of CO_2 on immune responses. Further characterization of the candidate CO_2 mediators will be required to identify those that have instructive rather than permissive roles in responses to elevated CO_2.

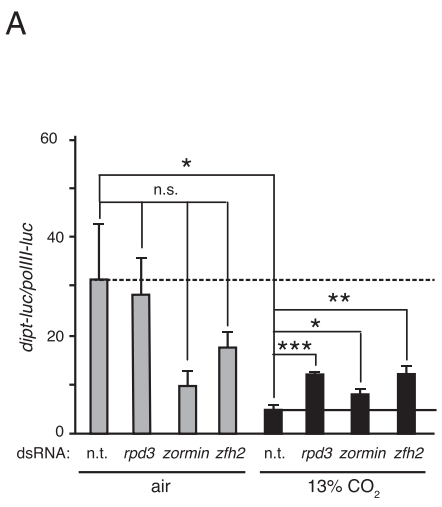

B

Fly gene	ortholog	function	CO_2 / air [dsRNA] low	high
zormin	Titin	muscle, chromatin	3.5	7.1
zfh2	ZFHX3/4	transcription factor	3.4	4.7
flfl	SMEK2	Protein phosphatase regulatory subunit 3	3.8	3.1
CG8239	MVD	mevalonate decarboxylase	2.1	4.7
mfr	-	synaptic vesicle exocytosis	3.6	2.9
ras85d	KRas	small GTPase	3.4	3.1
rhogap15b	ARAP1/2/3	rho family GAP	2.9	2.8
scaf6	CHERP	predicted mRNA binding	2.2	3.3
corin	SFRS1	scavenger receptor, ser-type endopeptidase	1.6	3.6
Rpd3	HDAC1	histone deacetylase	2.3	2.7
acox57d-d	ACOX1/2	acyl-CoA dehydrogenase	1.0	3.1
trx	KMT2A/B	histone methyltransferase	2.7	2.1
ced-6	GULP1	PTB domain	1.3	3.0
CG1271	GK5	carbohydrate kinase	2.1	2.2
gckIII	STK25	dual specificity prot. kinase	1.7	2.4
serT	SLC6A	neurotransmitter:Na⁺ symport	1.6	2.2
cycD	CCND2	cyclin	1.0	2.4

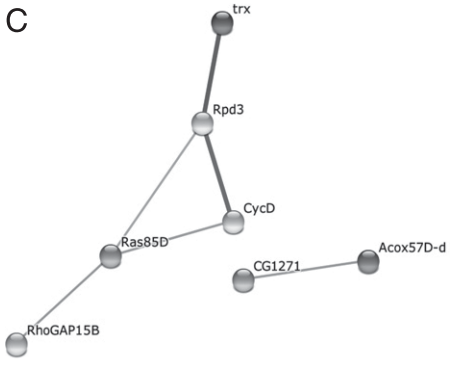

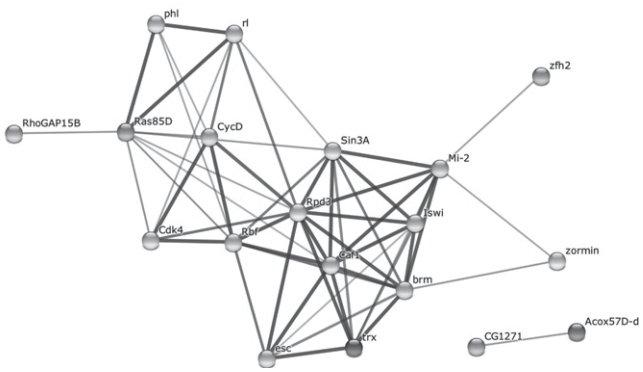

FIGURE 2. Secondary screening identifies putative CO_2-response mediator genes. (**A**) Normalized *Dipt-luc* reporter expression in control S2* cells and in cells treated with dsRNAs targeting *rpd3*, *zormin*, and *zfh2*. Dashed line indicates expression in control cells in air; solid line indicates expression in control cells in 13% CO_2 in pH 7.1 media. n.t., control nontargeting dsRNA. Statistical significance was determined using a Student *t* test: $*p < 0.05$, $**p < 0.01$, $***p < 0.001$. (**B**) The ratio of the expression of the normalized *Dipt-luc* reporter in CO_2 versus air, for cells treated with dsRNAs at low and high concentrations. Shown are the 17 genes with the highest CO_2/air ratios. The results for all 39 candidate genes tested in air and CO_2 are shown in Supplemental Table III. (**C**) An interaction network of genes in (B) predicted by the STRING program (44) using medium confidence settings. A subset of candidate CO_2 mediators have previously identified interactions. (**D**) An interaction network of genes in (B) predicted by the STRING program with extended connections that include known interactions that could relate *zormin* and *zfh2* to other candidate CO_2 mediators.

zfh2 encodes a large conserved transcription factor expressed in S2 cells and adult* Drosophila

To begin validation of candidate effectors of CO_2-induced immune suppression, we selected *zfh2* for further analysis. *zfh2* was a strong candidate because two separate dsRNAs targeting *zfh2* in the primary screen had average *Z*-scores from duplicate plates in the top 10 of all dsRNAs (amplicons DRSC17178 and DRSC28010, Supplemental Table II), and further screening revealed robust upregulation of the *Dipt-luc* reporter upon *zfh2* knockdown in 13% CO_2 (3.9- and 2-fold at low and high dsRNA concentrations, respectively) but not in air (1.1- and 0.4-fold) (Fig. 2A, Supplemental Table III). Furthermore, as detailed below, *zfh2* encodes a transcription factor, which we expect to have a more specific role in CO_2 signal transduction than other candidate genes such as *trx* or *rpd3* that encode chromatin-modifying proteins. Finally, previous work on *zfh2* has generated important reagents, including mutant lines, UAS-RNAi lines, and Abs.

The *zfh2* gene encodes three isoforms of a large, ~330-kDa protein containing 13 zinc fingers and three homeodomains. Two of the isoforms, Zfh2-PA and Zfh2-PB, are 3003 and 3005 aa long, respectively, and differ by only two amino acids. A third isoform, Zfh2-PC, is generated by an alternative splice near the 3′ end of the coding sequence that truncates the C-terminal 200 aa of the A and B isoforms, including part of the C-terminal homeodomain (Fig. 3A). The amplicons and UAS-RNAi constructs used in the RNAi screen and in vivo assays (see below) target all splice forms of *zfh2*. Zfh2 is part of a large family of zinc finger homeodomain proteins present in most metazoans (Fig. 3B) (46), with the two clearest human orthologs of Zfh2 being ZFHX3 (also known as ATBF1, ATBT, ZNF927) (47–54) and ZFHX4 (55–57). Human ZFHX3 and ZFHX4 also encode large ~400-kDa proteins containing 23 zinc fingers and four homeodomains (Fig. 3A, 3B). Zfh2 is 25 and 24% identical to ZFHX3 and ZFHX4, respectively (58). The first three homeodomains of ZFHX3 share 77, 69, and 61% identity with the corresponding homeodomains of Zfh2, and several of the zinc finger motifs in ZFHX3 and Zfh2 share 52–71% identity (59). Notably, the 200 aa deleted in the Zfh2-PC isoform have 30% similarity to the C termini of ZFHX3 and ZFHX4, suggesting that Zfh2-PC may have significant functional differences from Zfh2-PA and Zfh2-PB. A third potential human ortholog of Zfh2 is ZFHX2, but ZFHX2 appears to be further diverged from Zfh2 than either ZFHX3 or ZFHX4, sharing only 16% amino acid identity with *Drosophila* Zfh2 (58). Furthermore, using the DIOP ortholog search tool (60), ZFHX2 is identified as a Zfh2 ortholog by only three of nine prediction programs (Homologene, Inparanoid, Isobase, OMA, OrthoDB, OrthoMCL, Phylome, RoundUp, TreeFam), wherea ZFHX3 and ZFHX4 are identified by seven and six databases, respectively. *zfh2* has previously been shown to have an important role in neural and epithelial development and in regulating cell death (27, 61–65).

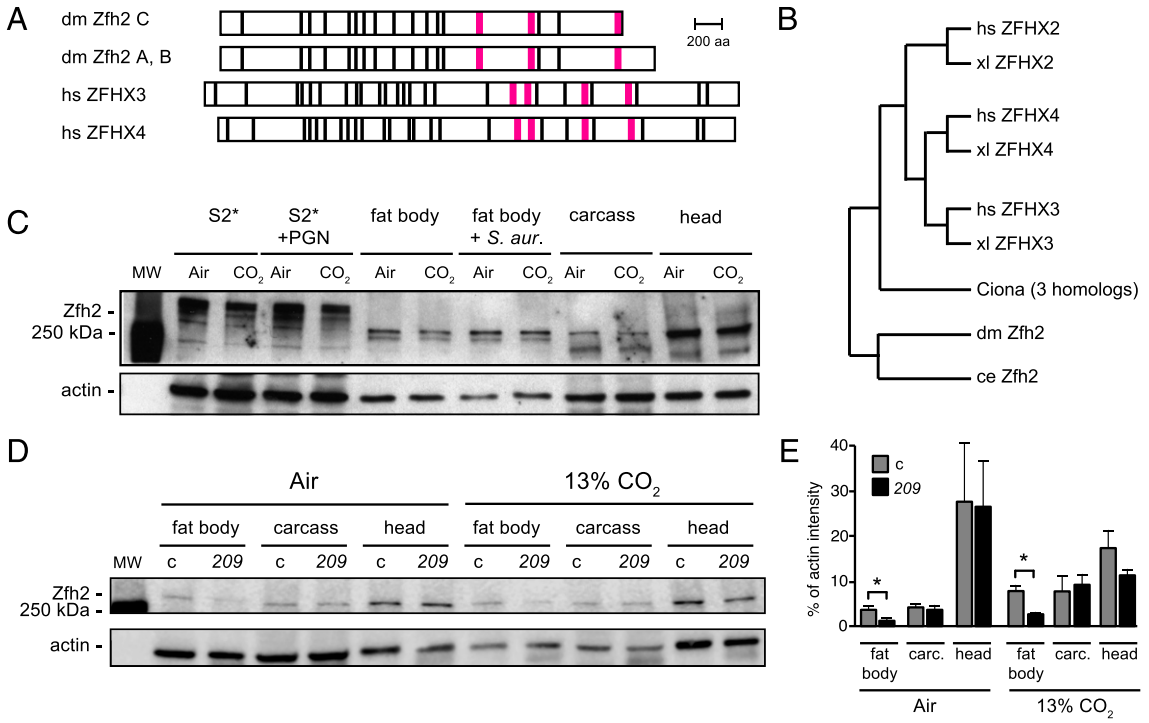

FIGURE 3. *zfh2* encodes a large conserved transcription factor expressed in immune tissues. (**A**) Domain structure of *Drosophila* (dm) Zfh2 isoforms A, B, and C, and human (hs) ZFHX3 and ZFHX4. Zfh2 isoforms A and B differ by only 2 aa and are shown together. Black bar indicates predicted zinc finger; magenta bar indicates predicted homeodomain. (**B**) A phylogenetic tree showing the relationships between *Drosophila* (dm) Zfh2 and human (hs), xenopus (xl), Ciona, and *C. elegans* (ce) zinc finger homeodomain proteins. The tree was generated using Ensembl release 81, June 2015 (76), which does not use branch length to represent evolutionary distance. (**C**) Western blot using rat polyclonal anti-Zfh2 antiserum (33) shows that Zfh2 is expressed strongly in neural tissue (head) and at lower, but easily detectable, levels in the fat body and the S2* cell line. Zfh2 levels in S2* cells and all tissues appear similar following exposure to air or 13% CO_2 and after immune challenge (PGN for S2* cells, *S. aureus* inoculation for adult flies; see *Materials and Methods*). Actin was used as the loading control; carcass indicates remaining fly body after removal of the head and the abdominal fat body; fat body indicates fat body tissue dissected from the abdomens of adult flies (20/lane). (**D**) Western blot comparing Zfh2 expression in the fat bodies, carcasses, and heads of control (c) and $zfh2^{MS209}$ (*209*) mutant flies. Blot was performed using rat polyclonal anti-Zfh2 antiserum (33), with chemiluminescence detection imaged by an Odyssey Fc imaging system (LI-COR Biosciences). Shown blot is representative of triplicate experiments. (**E**) Quantification of the bands from the Western blot in (D) and two replicates using the LI-COR Odyssey imaging system reveals that in $zfh2^{MS209}$ flies (*209*), Zfh2 levels are reduced ~2-fold in the fat body, but similar in the carcass and head, compared with control flies (c, w^{1118}). carc., carcass. $*p < 0.05$.

ZFHX3 is involved in neural and epithelial development (47–50), implicated by GWAS in atrial fibrillation (51), and it has roles in multiple types of cancer (52–54). Similarly, ZFHX4 is involved in epithelial and glial cancers (55, 56) and in neuronal development (57). However, neither Zfh2 nor its human orthologs ZFHX3 and ZFHX4 had previously been shown to regulate immune gene transcription or gas sensing. Taken together, these observations suggest that Zfh2, ZFHX3, and ZFHX4 could define a family of conserved, but previously unidentified, proteins that mediate hypercapnic immune suppression.

To investigate a potential role for Zfh2 in immune regulation, we determined where Zfh2 was expressed and whether its levels were altered by immune stimulation or by hypercapnia. FlyBase listed Zfh2 as being enriched in the nervous system and not expressed significantly in other tissues or S2 cells (66). Western blotting (Fig. 3C) confirmed strong expression of Zfh2 in neural tissue (adult fly heads), and in addition revealed Zfh2 expression in both S2* cells and in the adult abdominal fat body, the major immune and metabolic organ in *Drosophila*. In adult flies, a predominant band of Zfh2 immunostaining at ~300 kDa is observed; however, lower molecular mass bands are also present. In S2* cells, multiple higher molecular mass bands are observed that appear considerably >300 kDa. The larger molecular mass bands may represent posttranslationally modified Zfh2, because they are strongly reduced in RNAi and CRISPR experiments, but are not consistent with the predicted sizes of Zfh2 isoforms (Supplemental Fig. 1). PGN challenge of S2* cells and *S. aureus* infection of adult flies did not appear to alter Zfh2 protein levels or electrophoretic mobilities (Fig. 3C). Likewise, exposure to 13% CO_2, as compared with air, did not dramatically alter Zfh2 protein levels in S2* cells or adult fly tissues (Fig. 3C–E).

Zfh2 is required for elevated CO_2 levels to decrease resistance to bacterial infection in vivo

To determine whether Zfh2 mediates hypercapnic immune suppression in vivo, we tested whether *zfh2* mutant files were protected from the increase in mortality caused by elevated CO_2 in an *S. aureus* infection assay (Fig. 4A; see *Materials and Methods*). We were unable to assess the impact of complete Zfh2 deficiency because flies homozygous for strong *zfh2* mutations, such as $zfh2^{1\text{-}M707.R}$ (27), do not survive to adulthood (data not shown). Transheterozygous combinations of $zfh2^{1\text{-}M707.R}$ and weaker alleles, such as $zfh2^{MS209}$ (27), are also not viable as adults (data not shown). However, we were able to analyze animals homozygous for the $zfh2^{MS209}$ mutation, which is a hypomorphic allele resulting from a transposon insertion in the 3′ region of *zfh2* (67). $zfh2^{MS209}$ homozygotes have wing and leg developmental defects (67), but are viable for use in infection assays. $zfh2^{MS209}$ mutant flies (w^{1118};$zfh2^{MS209}$) and control flies (w^{1118}) maintained in air experience approximately the same mortality postinfection with *S. aureus* (Fig. 4B; red $zfh2^{MS209}$ line above and below black control line, $p = 0.18$). However, when exposed to 13% CO_2 for 48 h prior to infection, $zfh2^{MS209}$ mutants exhibit significantly reduced mortality compared with w^{1118} controls (Fig. 4C; red $zfh2^{MS209}$ line above black w^{1118} control line, $p < 0.0005$). Note that flies were exposed to elevated CO_2 before infection only and placed in air after infection to avoid confounding effects of simultaneously exposing the pathogen as well as the host to hypercapnia. Consistent with the fact that $zfh2^{MS209}$ is a partial loss-of-function mutation, Zfh2 levels in $zfh2^{MS209}$ homozygotes are not different from control flies in the head and carcass, but are reduced ~2-fold in the fat body (Fig. 3D, 3E, 4F). $zfh2^{MS209}$ mutants are not completely protected from the increased postinfection mortality caused by elevated CO_2 (Fig. 4D, $p = 0.009$), although the deleterious effect of hypercapnia is less than in control flies (compare Fig. 4A and 4D). Thus, mutation of *zfh2* allows flies to better survive infection after exposure to hypercapnia.

We next investigated whether the improved survival of hypercapnia-exposed $zfh2^{MS209}$ flies resulted from increased resistance (the ability to limit pathogen burden) (68), or increased tolerance (the ability to limit the health impact of a given pathogen burden) (68), of the bacterial infection. The $zfh2^{MS209}$ mutation appears to increase resistance because hypercapnia leads to increased bacterial load in control animals, but not in $zfh2^{MS209}$ homozygotes (Fig. 4E). Taken together, these results indicate that *zfh2* is required for CO_2 to suppress antibacterial host defense in vivo.

To confirm the above results and to identify tissues in which *zfh2* acts to mediate CO_2-induced immune suppression, we used the GAL4/UAS system (69) to express a *zfh2*-targeted short hairpin RNA construct (31) under the control of tissue-specific drivers. Consistent with the lethal phenotype of strong *zfh2* mutations, *da-GAL4*–driven ubiquitous expression of the *zfh2* RNAi construct $UAS\text{-}zfh2^{13305}$ caused lethality during embryonic and larval stages, and no pupa were observed (data not shown). However, embryonic, larval, and pupal development were not overtly perturbed by using the *CG-GAL4* or *C754-GAL4* drivers to express $UAS\text{-}zfh2^{13305}$ in the fat body, the major AMP-producing organ in the fly. Importantly, *CG-GAL4*–driven knockdown of *zfh2* by $UAS\text{-}zfh2^{13305}$ reduces Zfh2 protein levels in the fat body, but not the rest of the body or head (Fig. 4F), and it provides protection against hypercapnic immune suppression (Fig. 4I). Whereas exposure to 13% CO_2 increases mortality of *S. aureus* infection in *CG-GAL4* control adults (Fig. 4H; red CO_2 line below the black air line, $p = 0.0001$ for *CG-GAL4*/*CG-GAL4*; $p = 0.03$ for *CG-GAL4*/+, data not shown), hypercapnia does not increase the mortality of infection in $zfh2^{13305}$/*CG-GAL4* adults (Fig. 4I; red CO_2 line superimposed on black air line, $p = 0.44$). Expression of UAS-$zfh2^{13305}$ using another fat body driver, *C754-GAL4*, also improved survival of infected flies exposed to elevated CO_2 (Fig. 4J, 4K). Improved survival of adult flies with fat body–specific knockdown of *zfh2* is due at least in part to increased resistance to infection because bacterial load in UAS-$zfh2^{13305}$/*CG-GAL4* was not increased in flies exposed to 13% CO_2 compared with air (Fig. 4G). Importantly, no difference in bacterial loads was observed between control flies and flies with reduced Zfh2 levels in the fat body exposed to air alone (Fig. 4G), indicating that Zfh2 is not a major regulator of immune responses in ambient air. Taken together, to our knowledge, these results identify Zfh2 as the first in vivo mediator of hypercapnic immune suppression. Furthermore, the data provide strong evidence that the immunosuppressive effects of hypercapnia in *Drosophila* are mediated by a specific genetic pathway that functions in the fat body.

Zfh2 influences a nonimmunological function affected by hypercapnia

We next asked whether Zfh2 was a global mediator of hypercapnic responses, or whether it acted specifically in the immune system. We assayed the ability of *zfh2* mutations to prevent the hypercapnia-induced reductions in egg laying and delays in hatching that we had previously observed (21). The partial loss-of-function $zfh2^{MS209}$ and $zfh2^{2\text{-}M390.R}$ mutations do not significantly alter the suppression of egg laying by 13 or 19.5% CO_2 (Fig. 5A), but they can partially mitigate the delay in egg hatching by 24 h in 13% CO_2 and by 48 h in 19.5% CO_2 (Fig. 5B, 5C). These results provide evidence that *zfh2* mediates additional deleterious effects of elevated CO_2 on a process not directly related to immune function in tissues other than the fat body.

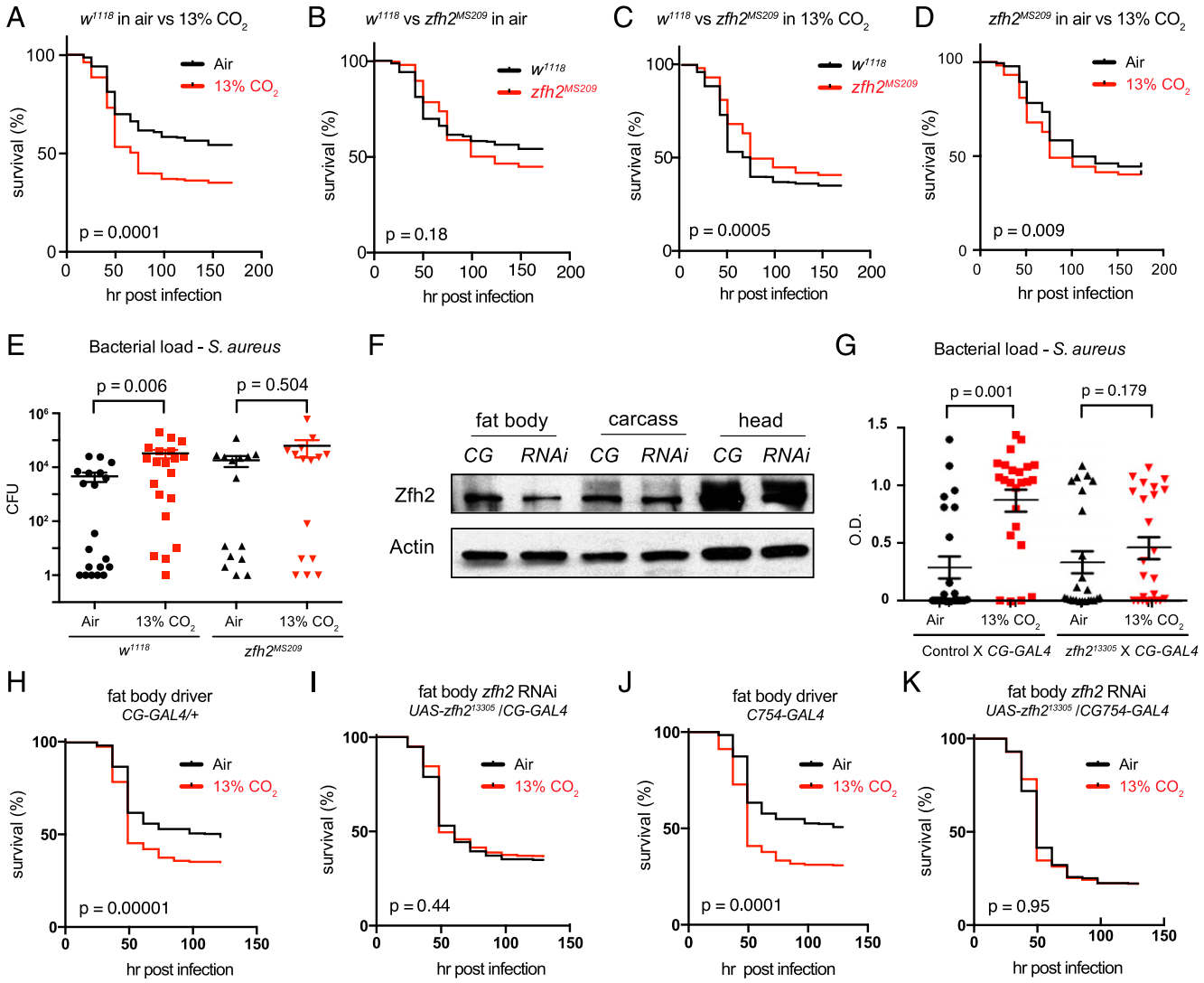

FIGURE 4. *zfh2* mediates hypercapnic immune suppression in vivo. (**A**) Control (w^{1118}) flies exposed to hypercapnia (13% CO_2) for 48 h, then inoculated with *S. aureus*, show reduced survival compared with *S. aureus*–infected flies exposed only to air (n = 636 for air, 622 for 13% CO_2). For mortality experiments, p values were calculated using the Gehan–Breslow–Wilcoxon test. (**B**) In air, mortality of *S. aureus* infection in $zfh2^{MS209}$ mutant flies is not different from in w^{1118} control flies (n = 636 for w^{1118}, 358 for w^{1118};$zfh2^{MS209}$). (**C**) When pre-exposed to 13% CO_2, $zfh2^{MS209}$ flies exhibit decreased mortality from *S. aureus* infection compared with w^{1118} control flies (n = 622 for w^{1118}, 336 for w^{1118};$zfh2^{MS209}$). (**D**) $zfh2^{MS209}$ flies are partially protected against the increase in mortality of *S. aureus* infection caused by exposure to elevated CO_2; genotype, w^{1118};$zfh2^{MS209}$ (n = 358 for air, 336 for 13% CO_2). [Compare to w^{1118} control flies in (A).] (**E**) Pre-exposure to 13% CO_2 increases bacterial load in w^{1118} but not w^{1118};$zfh2^{MS209}$ flies. Error bars show mean and SEM of the $\log_{10}$ load values (n = 20 for w^{1118} in air and 13% CO_2, 16 for $zfh2^{MS209}$ in air and CO_2). (**F**) Zfh2 protein levels are reduced in the fat body, but not the carcass or head, of flies with *CG-GAL4* driven expression of the *UAS-*$zfh2^{13305}$ short hairpin RNAi construct (RNAi; genotype w^{1118};*CG-GAL4/UAS-*$zfh2^{13305}$). CG, control genotype w^{1118};*CG-GAL4/+*. (**G**) Exposure to 13% CO_2 for 48 h prior to infection increases bacterial load in control (w^{1118};*CG-GAL4/+*) but not *CG-GAL4/UAS-*$zfh2^{13305}$ flies. Error bars show mean and SEM of the $\log_{10}$ load values (n = 24 for each condition). (**H**) Exposure to 13% CO_2 for 48 h prior to infection increases the mortality of *S. aureus* infection in control *CG-GAL4* flies (w^{1118};*CG-GAL4/+*) (n = 428 for air, 465 for 13% CO_2). (**I**) Exposure to 13% CO_2 for 48 h prior to infection does not increase mortality of *S. aureus* infection in flies in which *zfh2* was knocked down in the fat body (w^{1118};*CG-GAL4/UAS-*$zfh2^{13305}$) (n = 610 for air, 685 for 13% CO_2). (**J** and **K**) Results similar to those in (H) and (I) were obtained using another fat body–specific driver, *C754-GAL4* (n = 314 for control–air, 357 for control–13% CO_2, 459 for *C754-GAL4/UAS-*$zfh2^{13305}$–air, and 488 for *C754-GAL4/UAS-*$zfh2^{13305}$–13% CO_2).

Zfh2 mediates ex vivo hypercapnic suppression of multiple antimicrobial peptides

To determine whether increased expression of AMPs by the fat bodies of *zfh2* knockdown flies could be at least partially responsible for the improved survival of *zfh2* knockdown flies in elevated CO_2, we developed an ex vivo system for culturing fat bodies (see *Materials and Methods*). In this system, abdominal fat bodies are dissected from adult males and cultured in S2* media for 24 h in air or 13% CO_2. PGN treatment and media conditions were the same as for S2* cell culture, using fat bodies from three flies per experimental condition. In this assay, PGN causes a 4-fold induction of endogenous *Dipt* mRNA levels that is not suppressed by culture in pH 6.5 media, but is suppressed 3-fold by culture in 13% CO_2 (media pH 6.5) and 10-fold by culturing in 13% CO_2 in pH-neutralized media (pH 7.1, Fig. 6A).

When cultured in air, *Dipt* induction by PGN was not different in *zfh2* knockdown fat bodies than in control fat bodies (Fig. 6B). Notably, culture in 13% CO_2 at pH 6.5 did not reduce induction of *Dipt* in *zfh2* knockdown fat bodies (Fig. 6B), in marked contrast to results in control fat bodies (Fig. 6A). This finding corroborates

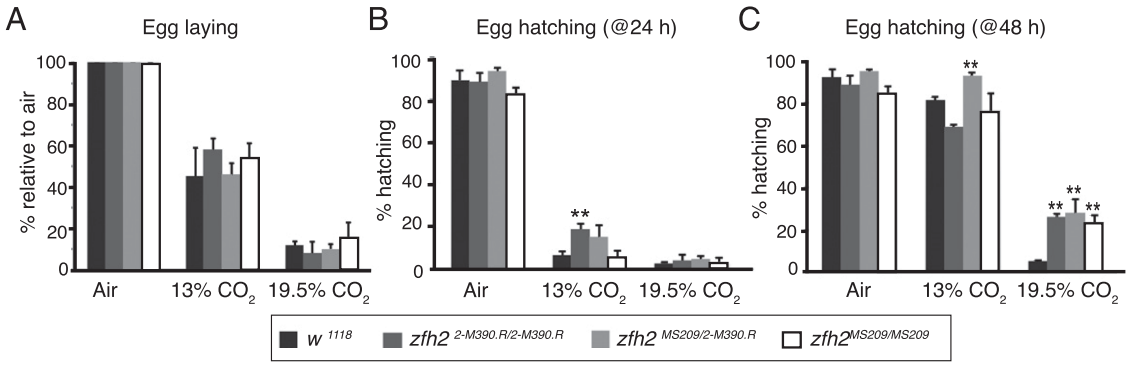

FIGURE 5. The partial loss-of-function mutations $zfh2^{MS209}$ and $zfh2^{2\text{-}M390.R}$ mitigate hypercapnia-induced reductions in egg hatching. (**A**) Flies homozygous for the partial loss-of-function mutations $zfh2^{2\text{-}M390.R}$ (dark gray) or $zfh2^{MS209}$ (white), or the transheterozygous combination of $zfh2^{2\text{-}M390.R}$ and $zfh2^{MS209}$ (light gray), are not protected from the suppressive effect of 13% CO_2 on egg laying seen in control animals (w^{1118}, black). All *zfh2* genotypes are w^{1118};*zfh2*. (n = 998 for w^{1118}, 243 for $zfh2^{2\text{-}M390.R}$, 440 for $zfh2^{2\text{-}M390.R/MS209}$, 195 for $zfh2^{MS209}$). (**B** and **C**) Hypercapnic suppression of egg hatching is attenuated in *zfh2* mutants flies. $^{**}p < 0.01$ using Student t test compared with w^{1118} for each condition. For (B), n = 821 for w^{1118}, 488 for $zfh2^{2\text{-}M390.R}$, 408 for $zfh2^{2\text{-}M390.R/MS209}$, and 130 for $zfh2^{MS209}$; for (C), n = 845 for w^{1118}, 682 for $zfh2^{2\text{-}M390.R}$, 350 for $zfh2^{2\text{-}M390.R/MS209}$, and 207 for $zfh2^{MS209}$.

the protective effect of *zfh2* knockdown in the infection assays (Fig. 4I, 4K) and the CO_2-specific increases in *Dipt-luc* expression observed in *zfh2* RNAi-treated S2* cells (Fig. 2). Culture of *zfh2* knockdown fat bodies in 13% CO_2 in media buffered to pH 7.1 did reduce *Dipt* induction compared with culture in air; however, the reduction was significantly less than in control fat bodies, with *zfh2* knockdown fat bodies inducing *Dipt* 3.6-fold more than control fat bodies under these culture conditions (Fig. 6B). Thus, Zfh2 mediates an immune suppressive effect of elevated CO_2 on induction of *Dipt* transcription that is not dependent on extracellular acidosis.

To investigate whether Zfh2 regulates expression of AMPs other than *Dipt*, we determined the effects of *zfh2* knockdown on *Att* and *Cec*, which can be induced by the Imd/Rel pathway (70), *Drs*, which is predominantly induced by the Toll pathway (71), and *Mtk*), which can be induced by both the Imd and Toll family receptors (71). Whereas knockdown of *zfh2* had no effect on PGN-stimulated induction of these AMPs in fat bodies cultured ex vivo in air (Fig. 6D), *zfh2* knockdown significantly attenuated hypercapnic suppression of *Att* and *Mtk,* in addition to *Dipt* (Fig. 6E), in fat bodies cultured in 13% CO_2. Knockdown of *zfh2* may have also attenuated hypercapnic suppression of *Cec*; however, *Cec* mRNA levels were more variable than those of the other AMPs, such that the increase in expression in CO_2 relative to air did not reach statistical significance (Fig. 6E). Expression of *Drs* in elevated CO_2 was not affected by *zfh2* knockdown (Fig. 6E), but as *Drs* was not actually induced by PGN (Fig. 6D), this experiment does not address whether *zfh2* modulates induction of genes by the Toll pathway. However, the results do indicate that Zfh2 does not control baseline (uninduced) levels of at least one Toll-regulated gene. Taken together, these findings demonstrate that *zfh2* mediates hypercapnic suppression of multiple Imd/Rel-regulated immune genes in the fat body, and that the suppressive effect of *zfh2* is specific to conditions of elevated CO_2.

The ex vivo fat body experiments also provided insight into the detrimental effects of *zfh2* knockdown in flies maintained in air, both in the absence and presence of infection. Flies in which *zfh2* has been knocked down in the fat body take ~4 d longer to reach adulthood than do control animals (data not shown), and mortality of *zfh2* fat body knockdown flies after infection in air is increased compared with controls (Fig. 4J, 4K). This may be explained by the finding that fat bodies from *zfh2* knockdown flies raised in air had smaller volumes than fat bodies from control flies. Also, induction of *Dipt* was reduced in *zfh2* knockdown fat bodies compared with control fat bodies, when cultured in air at pH 6.5 or at pH 7.1 with hypertonic media (25 mM NaCl) (Fig. 6C). Given the delayed growth of the *zfh2* knockdown flies and the adverse effects of culture in low pH or hypertonic media in air on *Dipt* induction in cultured fat bodies from these animals, it is striking that induction of *Dipt* in cultured *zfh2* knockdown fat bodies is not suppressed by elevated CO_2 and that *zfh2* knockdown in adult flies prevents 13% CO_2 from increasing the mortality of *S. aureus* infection. Taken together, these results show that Zfh2 has multiple functions in the adult fat body, one of which is to mediate the immunosuppressive effects of elevated CO_2.

Discussion

Although several CO_2 sensing pathways have been defined in neuronal tissues, it has largely been assumed that the nonneuronal physiological effects of CO_2 are exerted indirectly, either by H^+ and HCO^{3-} or by neuronal signaling. However, a growing body of evidence indicates that multiple nonneuronal cell types respond to elevated CO_2 levels under neutral pH conditions, and responses to CO_2 can be distinguished from responses to acidosis or bicarbonate (reviewed in Ref. 72). The molecular basis of these responses is a focus of current research, however, to date the mechanisms by which CO_2 influences immune systems have not been elucidated. In this study, we report a genome-wide RNAi screen that used *Drosophila* S2* cells to identify genes that mediate CO_2-induced suppression of Dipt, an important antimicrobial peptide. We identified 16 genes with human orthologs whose knockdown could cause the PGN-induced levels of a *Dipt* reporter to increase ≥2-fold more in 13% CO_2 than in air. In vivo analysis of one of these genes, which encodes the transcription factor Zfh2, demonstrates that reducing *zfh2* function in adult fat bodies by RNAi does not alter PGN-induced expression of AMP mRNAs during culture in air, but increases expression of *Dipt* and several other AMPs when cultured in elevated CO_2. Correspondingly, reducing *zfh2* function in whole flies by mutation, or more specifically in the fat body by RNAi knockdown, improves the ability of adult flies to clear and survive infection with *S. aureus*.

Implications of Zfh2 as a CO_2 mediator

The identification of Zfh2 as a CO_2 mediator is important for guiding further investigation of hypercapnic immune suppression in *Drosophila*. In particular, the ability of fat body–directed knockdown of *zfh2* to prevent hypercapnic immune suppression identifies a site of action for this CO_2 response pathway. Because

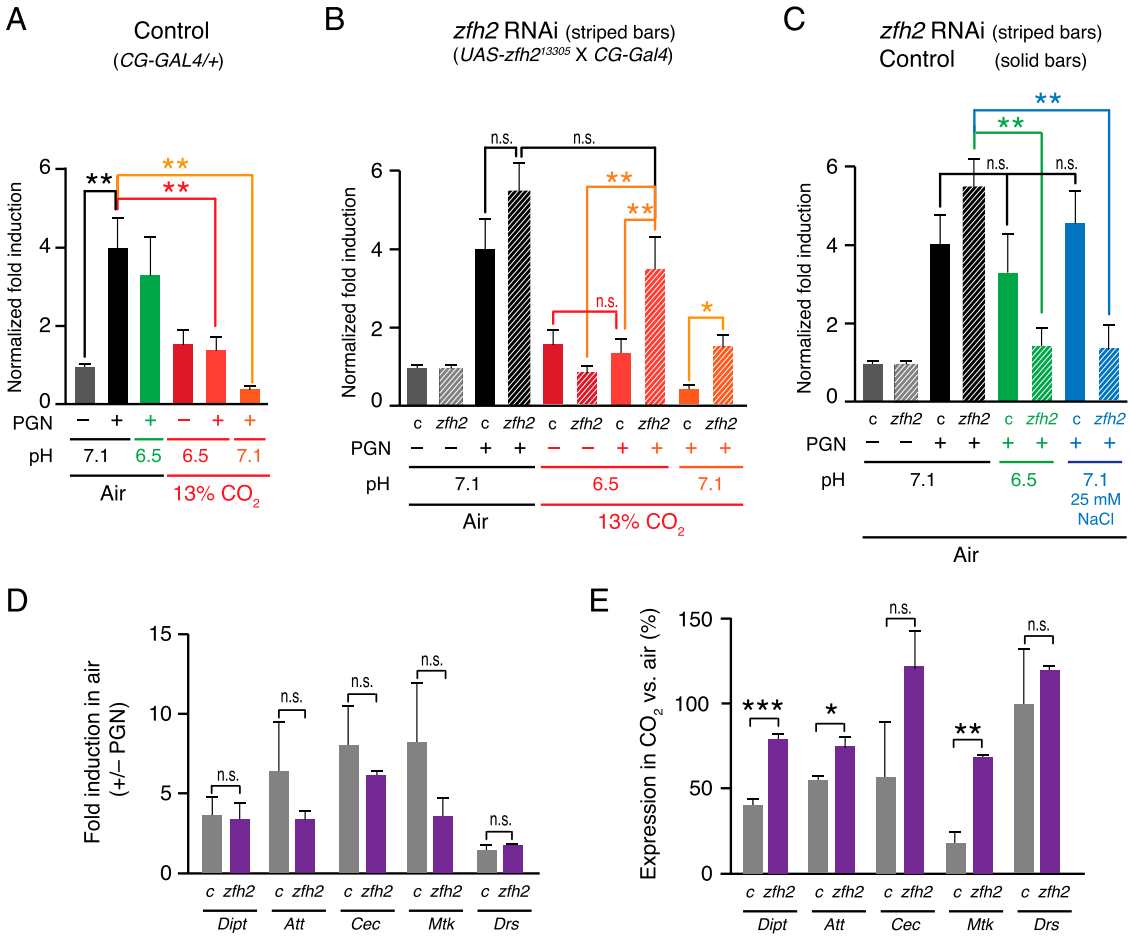

FIGURE 6. *zfh2* mediates hypercapnic suppression of AMPs in adult fat bodies cultured ex vivo. (**A**) Hypercapnia, but not normocapnic acidosis, suppresses *Dipt* induction in ex vivo cultured control fat bodies to a similar extent as does the suppression of *Dipt* induction observed in S2* cells (21). Bars show *Dipt* mRNA levels (normalized to RP49 mRNA) in fat bodies from control adults (w^{1118};*CG-Gal4/+*, solid bars) that have been cultured ex vivo in media equilibrated with air or 13% CO_2, uninduced and PGN-induced, at pH 7.1 (media without additions for air, or media plus 25 mM NaOH for 13% CO_2) or pH 6.5 (media plus 19 mM MOPS for air, or media without additions for 13% CO_2). (**B**) Fat body–specific knockdown of *zfh2* does not significantly increase *Dipt* induction when fat bodies are cultured in media equilibrated with air, but does prevent or reduce hypercapnia-induced suppression of *Dipt* induction in fat bodies cultured in media equilibrated with 13% CO_2 at pH 6.5 or pH 7.1. (B) shows data from the same experiment as in (A), and in addition shows results obtained using fat bodies from adults in which *zfh2* had been knocked down using a UAS-shRNA construct and the fat body driver, *CG-Gal4* (genotype, w^{1118};*UAS-zfh2*^{13305}*/CG-Gal4*, stripped bars). (**C**) Induction of *Dipt* is suppressed in *zfh2* knockdown, but not control, fat bodies cultured in media equilibrated with air at pH 6.5 or supplemented with 25 mM NaCl. (**D**) *zfh2* knockdown (purple bars) does not alter induction of *Dipt*, *Att*, *Cec*, or *Mtk* mRNAs in ex vivo–cultured fat bodies cultured in media equilibrated with air (gray bars, control [c], w^{1118};*CG-Gal4/+*; purple bars, *zfh2* knockdown, w^{1118};*UAS-zfh2*^{13305}*/CG-Gal4*). $n = 3$. (**E**) *zfh2* knockdown attenuates hypercapnic suppression of PGN-induced mRNA for *Dipt*, *Att*, and *Mtk* in ex vivo–cultured fat bodies. AMP mRNA levels in fat bodies cultured in 13% CO_2 in neutral media (pH7.1) are expressed as a percentage of the corresponding mRNA level in fat bodies cultured in air. For example, *Mtk* was suppressed ~80% by hypercapnia in control fat bodies, but only ~25% in *zfh2* knockdown fat bodies. Note that *Drs*, the expression of which is not suppressed by 13% CO_2, was not induced by PGN (D). Genotypes: same as in (D). $n = 3$. $^*p < 0.05$, $^{**}p < 0.01$, $^{***}p < 0.001$.

the fat body is the major immune organ of the fly, it is not surprising that it is an important target site of action for immunomodulatory effects of CO_2; however, it was nonetheless critical to establish this fact experimentally. Moreover, when combined with conditional knockdown tools (31, 69), identification of a site of action enables the study of other putative CO_2 response genes that have essential roles in embryonic development and thus are difficult or impossible to study in simple homozygous mutants.

Identification of Zfh2 is also a critical step in understanding the molecular mechanisms of hypercapnic immune suppression. *zfh2* knockdown in vivo almost fully rescues resistance to bacterial infection during hypercapnia, thus identifying *zfh2* as a major mediator of hypercapnic immune suppression. In S2* cells and in ex vivo fat bodies, knockdown of *zfh2* can eliminate up to 50% of the effect of elevated CO_2 on *Dipt* induction, suggesting that hypercapnia suppresses *Dipt* by acting on one or a small number of signaling pathways rather than by nonspecific mechanisms affecting the activity of many targets. This hypothesis is bolstered by our finding that increases in *Dipt* expression resulting from *zfh2* knockdown are specific for hypercapnia and do not occur during culture in air or in acidified media without hypercapnia. *zfh2* knockdown in fat bodies not only fails to mitigate the effects of nonhypercapnic acidosis, it makes fat bodies more sensitive to acidosis and less sensitive to elevated CO_2 levels. An important implication of the suggestion that the immune suppressive effects of hypercapnia are mediated by one or a small number of pathways is that, in principle, it should be possible to therapeutically block the effects of elevated CO_2 using small molecules.

Perhaps the most important aspect of the identification of Zfh2 as a mediator of hypercapnic immune suppression is that it may

provide an entry point to understanding the molecular mechanism of hypercapnic immune suppression in humans. Zfh2 has established orthologs in mammals, and we have previously shown that there are strong parallels between hypercapnic immune suppression in *Drosophila* and mammals (15, 16, 21). Although it is possible that Zfh2 acquired a role as a CO_2 mediator after flies and mammals diverged, strong conservation of the innate immune pathways, other gas-sensing pathways, as well as most other signaling systems, suggests that mammalian ZFHX3 and/or ZFHX4 could also mediate immunomodulatory effects of CO_2. Additionally, given that *zfh2* mutations partially blocked the effects of elevated CO_2 on egg hatching, it is also possible that ZFHX3 and ZFHX4 could act outside the immune system to mediate nonimmunological effects of elevated CO_2, such as hypercapnia-induced muscle wasting (73).

Possible models for how Zfh2 acts

How does Zfh2 mediate hypercapnic immune suppression? Zfh2 has 13 zinc fingers and three homeodomains, and it has been demonstrated to bind DNA. Although it is therefore likely that Zfh2 acts as a transcription factor in transducing CO_2 responses, zinc fingers can also mediate protein–protein interactions, raising the possibility that a nontranscriptional function of Zfh2 mediates CO_2 responses. In either case, the genetic data are consistent with Zfh2 acting as a CO_2-specific negative regulator of AMP induction, either by directly binding AMP promoters or by binding and inhibiting positive regulators of AMP induction. At this point, it is unclear whether Zfh2 is the sole mediator of the immunosuppressive effects of CO_2 because the lethality of Zfh2 mutants made it impossible to completely remove Zfh2 function. However, it seems likely that additional CO_2-responsive factors may suppress innate immune function in flies because the limited role of Zfh2 in CO_2-induced suppression of egg laying indicates that other CO_2-responsive pathways exist, and few immunological responses are regulated by a single pathway.

Zinc finger homeodomain proteins: a family of immune regulators?

In addition to *zfh2*/ZFHX3/ZFHX4, the *Drosophila* and human genomes encode a second family of zinc finger homeodomain–containing proteins (46). Members of this family, which includes *Drosophila zfh1* and human ZEB1 and ZEB2, are about one third the size of the Zfh2/ZFHX3/ZFHX4 protein family (~1100 aa), and each contains one homeodomain and seven to nine zinc finger domains. Notably, despite the considerable evolutionary divergence between these families, both Zfh1 and ZEB1 have been shown to also modulate NF-κB–regulated innate immune responses (74). Similar to Zfh2, Zfh1 is a negative regulator of *Dipt* and other Imd-responsive AMPs, including *Att* and *Cec*. Interestingly, epistasis experiments indicated that Zfh1 acts downstream of or in parallel to Rel, similar to our findings that elevated CO_2, apparently via Zfh2, suppresses AMPs downstream of Rel proteolytic activation (21). However, a critical difference between Zfh1 and Zfh2 is that whereas knockdown of *zfh1* in normocapnia increases expression of multiple AMPs, knockdown of *zfh2* only increases AMP expression in hypercapnia. These findings raise the possibility that an ancestral zinc finger homeodomain protein may have regulated immune responses, with the Zfh1/ZEB1/ZEB2 family evolving as general immune regulators, whereas Zfh2, and potentially other members of the Zfh2 family, evolved as CO_2-responsive regulators of innate immune responses. This specialization also suggests that the ability to separately regulate immune responses in normocapnia and hypercapnia is biologically important.

Was an immunomodulatory CO_2 sensor identified by the screen?

An interesting question is whether the screen identified a CO_2 sensor that controls hypercapnic immune suppression. The variety in known CO_2 sensing mechanisms, particularly the recent identification of a connexin subunit as a CO_2 sensor by carbamylation (75), indicates that, in principle, almost any protein could act as a sensor, thus making it difficult to predict CO_2 sensing ability based on known function or sequence. Thus, the screen may well have identified the sensor, but we are unable to recognize it as such at this time. Although it is possible that Zfh2 is carbamylated in elevated CO_2 levels and thus is both a sensor and effector, another likely scenario is that CO_2 levels are sensed by an as yet unidentified upstream pathway component, leading to posttranslational modification of Zfh2 that alters its capacity for DNA binding or protein–protein interactions, thereby altering transcription of AMPs and possibly other immune genes. Alternatively, secondary screening may not have identified the CO_2 sensor because we focused on dsRNAs whose knockdown in air had minimal effects, but in hypercapnia prevented suppression of *Dipt-luc*. If the sensor, or any part of a hypercapnia response pathway, is essential for Imd pathway signaling in air, it would not have scored as a positive in the screen. Further analysis of the hits from this screen, and the use of confirmed CO_2 mediators in assays of pathway function, will ultimately define the pathway of hypercapnic immune suppression and the CO_2 sensor that regulates it.

In conclusion, the goal of this work was to identify genes that mediate immune suppressive effects of hypercapnia. Our in vitro screen identified 16 candidate *Drosophila* CO_2 mediator genes that have human orthologs, one of which was tested for immunomodulatory effects in adult flies. These experiments defined Zfh2, to our knowledge, as the first known mediator of hypercapnic immune suppression. The screen was also expected to identify components of the Imd pathway that regulates the Dipt product, and given that 12 previously known positive and negative regulators of the Imd pathway were identified, it is likely that several of the candidate CO_2 mediators will be in vivo mediators of hypercapnic immune suppression. Thus, this screen is an important starting point in the quest to fully define the components of the signaling pathways that mediate hypercapnic immune suppression.

Acknowledgments

We thank the staff of the Northwestern High Throughput Analysis Laboratory and Harvard DRSC, in particular Sara Fernandez Dunne and Chi-Hao Luan (Northwestern University High Throughput Analysis Laboratory) and Stephanie Mohr and Quentin Gilly (Harvard DRSC), for technical assistance. We also thank Emilia Lecuona and Neal Silverman for advice; Chris Doe for anti-Zfh2 antisera; and the Bloomington *Drosophila* Stock Center, the Transgenic RNAi Project at Harvard Medical School, and Sarah Elgin for fly stocks.

Disclosures

The authors have no financial conflicts of interest.

References

1. Miniño, A. M. 2013. Death in the United States, 2011. *NCHS Data Brief* 2013 (115): 1–8.
2. Sethi, S., and T. F. Murphy. 2008. Infection in the pathogenesis and course of chronic obstructive pulmonary disease. *N. Engl. J. Med.* 359: 2355–2365.
3. Moser, K. M., E. M. Shibel, and A. J. Beamon. 1973. Acute respiratory failure in obstructive lung disease. Long-term survival after treatment in an intensive care unit. *JAMA* 225: 705–707.
4. Martin, T. R., S. W. Lewis, and R. K. Albert. 1982. The prognosis of patients with chronic obstructive pulmonary disease after hospitalization for acute respiratory failure. *Chest* 82: 310–314.

5. Goel, A., R. G. Pinckney, and B. Littenberg. 2003. APACHE II predicts long-term survival in COPD patients admitted to a general medical ward. *J. Gen. Intern. Med.* 18: 824–830.
6. Groenewegen, K. H., A. M. Schols, and E. F. Wouters. 2003. Mortality and mortality-related factors after hospitalization for acute exacerbation of COPD. *Chest* 124: 459–467.
7. Köhnlein, T., W. Windisch, D. Köhler, A. Drabik, J. Geiseler, S. Hartl, O. Karg, G. Laier-Groeneveld, S. Nava, B. Schönhofer, et al. 2014. Non-invasive positive pressure ventilation for the treatment of severe stable chronic obstructive pulmonary disease: a prospective, multicentre, randomised, controlled clinical trial. *Lancet Respir. Med.* 2: 698–705.
8. Wedzicha, J. A., and T. A. Seemungal. 2007. COPD exacerbations: defining their cause and prevention. *Lancet* 370: 786–796.
9. Bafadhel, M., S. McKenna, S. Terry, V. Mistry, C. Reid, P. Haldar, M. McCormick, K. Haldar, T. Kebadze, A. Duvoix, et al. 2011. Acute exacerbations of chronic obstructive pulmonary disease: identification of biologic clusters and their biomarkers. *Am. J. Respir. Crit. Care Med.* 184: 662–671.
10. Beasley, V., P. V. Joshi, A. Singanayagam, P. L. Molyneaux, S. L. Johnston, and P. Mallia. 2012. Lung microbiology and exacerbations in COPD. *Int. J. Chron. Obstruct. Pulmon. Dis.* 7: 555–569.
11. Sin, D. D., S. F. Man, and T. J. Marrie. 2005. Arterial carbon dioxide tension on admission as a marker of in-hospital mortality in community-acquired pneumonia. *Am. J. Med.* 118: 145–150.
12. Laserna, E., O. Sibila, P. R. Aguilar, E. M. Mortensen, A. Anzueto, J. M. Blanquer, F. Sanz, J. Rello, P. J. Marcos, M. I. Velez, et al. 2012. Hypocapnia and hypercapnia are predictors for ICU admission and mortality in hospitalized patients with community-acquired pneumonia. *Chest* 142: 1193–1199.
13. Murtagh, P., V. Giubergia, D. Viale, G. Bauer, and H. G. Pena. 2009. Lower respiratory infections by adenovirus in children. Clinical features and risk factors for bronchiolitis obliterans and mortality. *Pediatr. Pulmonol.* 44: 450–456.
14. Belkin, R. A., N. R. Henig, L. G. Singer, C. Chaparro, R. C. Rubenstein, S. X. Xie, J. Y. Yee, R. M. Kotloff, D. A. Lipson, and G. R. Bunin. 2006. Risk factors for death of patients with cystic fibrosis awaiting lung transplantation. *Am. J. Respir. Crit. Care Med.* 173: 659–666.
15. Wang, N., K. L. Gates, H. Trejo, S. Favoreto, Jr., R. P. Schleimer, J. I. Sznajder, G. J. Beitel, and P. H. Sporn. 2010. Elevated CO_2 selectively inhibits interleukin-6 and tumor necrosis factor expression and decreases phagocytosis in the macrophage. *FASEB J.* 24: 2178–2190.
16. Gates, K. L., H. A. Howell, A. Nair, C. U. Vohwinkel, L. C. Welch, G. J. Beitel, A. R. Hauser, J. I. Sznajder, and P. H. Sporn. 2013. Hypercapnia impairs lung neutrophil function and increases mortality in murine *Pseudomonas* pneumonia. *Am. J. Respir. Cell Mol. Biol.* 49: 821–828.
17. Casalino-Matsuda, S. M., A. Nair, G. J. Beitel, K. L. Gates, and P. H. Sporn. 2015. Hypercapnia inhibits autophagy and bacterial killing in human macrophages by increasing expression of Bcl-2 and Bcl-x_L. *J. Immunol.* 194: 5388–5396.
18. Cummins, E. P., K. M. Oliver, C. R. Lenihan, S. F. Fitzpatrick, U. Bruning, C. C. Scholz, C. Slattery, M. O. Leonard, P. McLoughlin, and C. T. Taylor. 2010. NF-κB links CO_2 sensing to innate immunity and inflammation in mammalian cells. *J. Immunol.* 185: 4439–4445.
19. Oliver, K. M., C. R. Lenihan, U. Bruning, A. Cheong, J. G. Laffey, P. McLoughlin, C. T. Taylor, and E. P. Cummins. 2012. Hypercapnia induces cleavage and nuclear localization of RelB protein, giving insight into CO_2 sensing and signaling. *J. Biol. Chem.* 287: 14004–14011.
20. Lardner, A. 2001. The effects of extracellular pH on immune function. *J. Leukoc. Biol.* 69: 522–530.
21. Helenius, I. T., T. Krupinski, D. W. Turnbull, Y. Gruenbaum, N. Silverman, E. A. Johnson, P. H. S. Sporn, J. I. Sznajder, and G. J. Beitel. 2009. Elevated CO_2 suppresses specific *Drosophila* innate immune responses and resistance to bacterial infection. *Proc. Natl. Acad. Sci. USA* 106: 18710–18715.
22. Vadász, I., L. A. Dada, A. Briva, I. T. Helenius, K. Sharabi, L. C. Welch, A. M. Kelly, B. A. Grzesik, G. R. Budinger, J. Liu, et al. 2012. Evolutionary conserved role of c-Jun-N-terminal kinase in CO_2-induced epithelial dysfunction. *PLoS One* 7: e46696.
23. Reichhart, J. M., M. Meister, J. L. Dimarcq, D. Zachary, D. Hoffmann, C. Ruiz, G. Richards, and J. A. Hoffmann. 1992. Insect immunity: developmental and inducible activity of the *Drosophila* diptericin promoter. *EMBO J.* 11: 1469–1477.
24. Tauszig, S., E. Jouanguy, J. A. Hoffmann, and J. L. Imler. 2000. Toll-related receptors and the control of antimicrobial peptide expression in *Drosophila*. *Proc. Natl. Acad. Sci. USA* 97: 10520–10525.
25. Nybakken, K., S. A. Vokes, T. Y. Lin, A. P. McMahon, and N. Perrimon. 2005. A genome-wide RNA interference screen in *Drosophila melanogaster* cells for new components of the Hh signaling pathway. *Nat. Genet.* 37: 1323–1332.
26. Ramadan, N., I. Flockhart, M. Booker, N. Perrimon, and B. Mathey-Prevot. 2007. Design and implementation of high-throughput RNAi screens in cultured *Drosophila* cells. *Nat. Protoc.* 2: 2245–2264.
27. Whitworth, A. J., and S. Russell. 2003. Temporally dynamic response to Wingless directs the sequential elaboration of the proximodistal axis of the *Drosophila* wing. *Dev. Biol.* 254: 277–288.
28. Sun, F. L., M. H. Cuaycong, C. A. Craig, L. L. Wallrath, J. Locke, and S. C. Elgin. 2000. The fourth chromosome of *Drosophila melanogaster*: interspersed euchromatic and heterochromatic domains. *Proc. Natl. Acad. Sci. USA* 97: 5340–5345.
29. Hennig, K. M., J. Colombani, and T. P. Neufeld. 2006. TOR coordinates bulk and targeted endocytosis in the *Drosophila melanogaster* fat body to regulate cell growth. *J. Cell Biol.* 173: 963–974.
30. Hrdlicka, L., M. Gibson, A. Kiger, C. Micchelli, M. Schober, F. Schöck, and N. Perrimon. 2002. Analysis of twenty-four Gal4 lines in *Drosophila melanogaster*. *Genesis* 34: 51–57.
31. Ni, J. Q., R. Zhou, B. Czech, L. P. Liu, L. Holderbaum, D. Yang-Zhou, H. S. Shim, R. Tao, D. Handler, P. Karpowicz, et al. 2011. A genome-scale shRNA resource for transgenic RNAi in *Drosophila*. *Nat. Methods* 8: 405–407.
32. Krupp, J. J., and J. D. Levine. 2010. Dissection of oenocytes from adult *Drosophila melanogaster*. *J. Vis. Exp.* (41):2242.
33. Tran, K. D., M. R. Miller, and C. Q. Doe. 2010. Recombineering Hunchback identifies two conserved domains required to maintain neuroblast competence and specify early-born neuronal identity. *Development* 137: 1421–1430.
34. Valanne, S., H. Myllymäki, J. Kallio, M. R. Schmid, A. Kleino, A. Murumägi, L. Airaksinen, T. Kotipelto, M. Kaustio, J. Ulvila, et al. 2010. Genome-wide RNA interference in *Drosophila* cells identifies G protein-coupled receptor kinase 2 as a conserved regulator of NF-κB signaling. *J. Immunol.* 184: 6188–6198.
35. Karhumaa, P., S. Parkkila, A. Waheed, A. K. Parkkila, K. Kaunisto, P. W. Tucker, C. J. Huang, W. S. Sly, and H. Rajaniemi. 2000. Nuclear NonO/$p54^{nrb}$ protein is a nonclassical carbonic anhydrase. *J. Biol. Chem.* 275: 16044–16049.
36. Misra, S., M. A. Crosby, C. J. Mungall, B. B. Matthews, K. S. Campbell, P. Hradecky, Y. Huang, J. S. Kaminker, G. H. Millburn, S. E. Prochnik, et al. 2002. Annotation of the *Drosophila melanogaster* euchromatic genome: a systematic review. *Genome Biol.* 3: research0083.1–83.22. doi:10.1186/gb-2002-3-12-research0083
37. Foley, E., and P. H. O'Farrell. 2004. Functional dissection of an innate immune response by a genome-wide RNAi screen. *PLoS Biol.* 2: E203.
38. Kleino, A., S. Valanne, J. Ulvila, J. Kallio, H. Myllymäki, H. Enwald, S. Stöven, M. Poidevin, R. Ueda, D. Hultmark, et al. 2005. Inhibitor of apoptosis 2 and TAK1-binding protein are components of the *Drosophila* Imd pathway. *EMBO J.* 24: 3423–3434.
39. Bond, D., and E. Foley. 2009. A quantitative RNAi screen for JNK modifiers identifies Pvr as a novel regulator of *Drosophila* immune signaling. *PLoS Pathog.* 5: e1000655.
40. Rämet, M., P. Manfruelli, A. Pearson, B. Mathey-Prevot, and R. A. Ezekowitz. 2002. Functional genomic analysis of phagocytosis and identification of a *Drosophila* receptor for *E. coli*. *Nature* 416: 644–648.
41. Choe, K. M., T. Werner, S. Stöven, D. Hultmark, and K. V. Anderson. 2002. Requirement for a peptidoglycan recognition protein (PGRP) in Relish activation and antibacterial immune responses in *Drosophila*. *Science* 296: 359–362.
42. Gottar, M., V. Gobert, T. Michel, M. Belvin, G. Duyk, J. A. Hoffmann, D. Ferrandon, and J. Royet. 2002. The *Drosophila* immune response against Gram-negative bacteria is mediated by a peptidoglycan recognition protein. *Nature* 416: 640–644.
43. Hedengren, M., B. Asling, M. S. Dushay, I. Ando, S. Ekengren, M. Wihlborg, and D. Hultmark. 1999. Relish, a central factor in the control of humoral but not cellular immunity in Drosophila. *Mol. Cell* 4: 827–837.
44. Franceschini, A., D. Szklarczyk, S. Frankild, M. Kuhn, M. Simonovic, A. Roth, J. Lin, P. Minguez, P. Bork, C. von Mering, and L. J. Jensen. 2013. STRING v9.1: protein-protein interaction networks, with increased coverage and integration. *Nucleic Acids Res.* 41: D808–D815.
45. Remm, M., C. E. Storm, and E. L. Sonnhammer. 2001. Automatic clustering of orthologs and in-paralogs from pairwise species comparisons. *J. Mol. Biol.* 314: 1041–1052.
46. Seetharam, A., Y. Bai, and G. W. Stuart. 2010. A survey of well conserved families of C2H2 zinc-finger genes in *Daphnia*. *BMC Genomics* 11: 276.
47. Jung, C. G., H. J. Kim, M. Kawaguchi, K. K. Khanna, H. Hida, K. Asai, H. Nishino, and Y. Miura. 2005. Homeotic factor ATBF1 induces the cell cycle arrest associated with neuronal differentiation. *Development* 132: 5137–5145.
48. Ishii, Y., M. Kawaguchi, K. Takagawa, T. Oya, S. Nogami, A. Tamura, Y. Miura, A. Ido, N. Sakata, T. Hashimoto-Tamaoki, et al. 2003. ATBF1-A protein, but not ATBF1-B, is preferentially expressed in developing rat brain. *J. Comp. Neurol.* 465: 57–71.
49. Miura, Y., T. Tam, A. Ido, T. Morinaga, T. Miki, T. Hashimoto, and T. Tamaoki. 1995. Cloning and characterization of an ATBF1 isoform that expresses in a neuronal differentiation-dependent manner. *J. Biol. Chem.* 270: 26840–26848.
50. Li, M., X. Fu, G. Ma, X. Sun, X. Dong, T. Nagy, C. Xing, J. Li, and J. T. Dong. 2012. Atbf1 regulates pubertal mammary gland development likely by inhibiting the pro-proliferative function of estrogen-ER signaling. *PLoS One* 7: e51283.
51. Zhou, M., Y. Liao, and X. Tu. 2015. The role of transcription factors in atrial fibrillation. *J. Thorac. Dis.* 7: 152–158.
52. Mori, Y., H. Kataoka, Y. Miura, M. Kawaguchi, E. Kubota, N. Ogasawara, T. Oshima, S. Tanida, M. Sasaki, H. Ohara, et al. 2007. Subcellular localization of ATBF1 regulates MUC5AC transcription in gastric cancer. *Int. J. Cancer* 121: 241–247.
53. Sun, X., X. Fu, J. Li, C. Xing, H. F. Frierson, H. Wu, X. Ding, T. Ju, R. D. Cummings, and J. T. Dong. 2014. Deletion of Atbf1/Zfhx3 in mouse prostate causes neoplastic lesions, likely by attenuation of membrane and secretory proteins and multiple signaling pathways. *Neoplasia* 16: 377–389.
54. Chen, D. B., and H. J. Yang. 2014. Comparison of gene regulatory networks of benign and malignant breast cancer samples with normal samples. *Genet. Mol. Res.* 13: 9453–9462.
55. Stacey, S. N., H. Helgason, S. A. Gudjonsson, G. Thorleifsson, F. Zink, A. Sigurdsson, B. Kehr, J. Gudmundsson, P. Sulem, B. Sigurgeirsson, et al. 2015. New basal cell carcinoma susceptibility loci. *Nat. Commun.* 6: 6825.
56. Chudnovsky, Y., D. Kim, S. Zheng, W. A. Whyte, M. Bansal, M. A. Bray, S. Gopal, M. A. Theisen, S. Bilodeau, P. Thiru, et al. 2014. ZFHX4 interacts with the NuRD core member CHD4 and regulates the glioblastoma tumor-initiating cell state. *Cell Reports* 6: 313–324.

57. Hemmi, K., D. Ma, Y. Miura, M. Kawaguchi, M. Sasahara, T. Hashimoto-Tamaoki, T. Tamaoki, N. Sakata, and K. Tsuchiya. 2006. A homeodomain-zinc finger protein, ZFHX4, is expressed in neuronal differentiation manner and suppressed in muscle differentiation manner. *Biol. Pharm. Bull.* 29: 1830–1835.
58. Cunningham, F., M. R. Amode, D. Barrell, K. Beal, K. Billis, S. Brent, D. Carvalho-Silva, P. Clapham, G. Coates, S. Fitzgerald, et al. 2015. Ensembl 2015. *Nucleic Acids Res.* 43: D662–D669.
59. Hashimoto, T., Y. Nakano, T. Morinaga, and T. Tamaoki. 1992. A new family of homeobox genes encoding multiple homeodomain and zinc finger motifs. *Mech. Dev.* 39: 125–126.
60. Hu, Y., I. Flockhart, A. Vinayagam, C. Bergwitz, B. Berger, N. Perrimon, and S. E. Mohr. 2011. An integrative approach to ortholog prediction for disease-focused and other functional studies. *BMC Bioinformatics* 12: 357.
61. Gabilondo, H., M. Losada-Pérez, D. del Saz, I. Molina, Y. León, I. Canal, L. Torroja, and J. Benito-Sipos. 2011. A targeted genetic screen identifies crucial players in the specification of the *Drosophila* abdominal Capaergic neurons. *Mech. Dev.* 128: 208–221.
62. Perea, D., K. Molohon, K. Edwards, and F. J. Díaz-Benjumea. 2013. Multiple roles of the gene zinc finger homeodomain-2 in the development of the *Drosophila* wing. *Mech. Dev.* 130: 467–481.
63. Terriente, J., D. Perea, M. Suzanne, and F. J. Díaz-Benjumea. 2008. The *Drosophila* gene *zfh2* is required to establish proximal-distal domains in the wing disc. *Dev. Biol.* 320: 102–112.
64. Lundell, M. J., and J. Hirsh. 1992. The *zfh-2* gene product is a potential regulator of neuron-specific dopa decarboxylase gene expression in *Drosophila*. *Dev. Biol.* 154: 84–94.
65. Guarner, A., C. Manjón, K. Edwards, H. Steller, M. Suzanne, and E. Sánchez-Herrero. 2014. The zinc finger homeodomain-2 gene of *Drosophila* controls Notch targets and regulates apoptosis in the tarsal segments. *Dev. Biol.* 385: 350–365.
66. dos Santos, G., A. J. Schroeder, J. L. Goodman, V. B. Strelets, M. A. Crosby, J. Thurmond, D. B. Emmert, and W. M. Gelbart, the FlyBase Consortium. 2015. FlyBase: introduction of the *Drosophila melanogaster* release 6 reference genome assembly and large-scale migration of genome annotations. *Nucleic Acids Res.* 43: D690–D697.
67. Capdevila, J., and I. Guerrero. 1994. Targeted expression of the signaling molecule decapentaplegic induces pattern duplications and growth alterations in *Drosophila* wings. *EMBO J.* 13: 4459–4468.
68. Schneider, D. S., and J. S. Ayres. 2008. Two ways to survive infection: what resistance and tolerance can teach us about treating infectious diseases. *Nat. Rev. Immunol.* 8: 889–895.
69. Brand, A. H., and N. Perrimon. 1993. Targeted gene expression as a means of altering cell fates and generating dominant phenotypes. *Development* 118: 401–415.
70. Tanji, T., X. Hu, A. N. Weber, and Y. T. Ip. 2007. Toll and IMD pathways synergistically activate an innate immune response in *Drosophila melanogaster*. *Mol. Cell. Biol.* 27: 4578–4588.
71. Valanne, S., J. H. Wang, and M. Rämet. 2011. The *Drosophila* Toll signaling pathway. *J. Immunol.* 186: 649–656.
72. Cummins, E. P., A. C. Selfridge, P. H. Sporn, J. I. Sznajder, and C. T. Taylor. 2014. Carbon dioxide-sensing in organisms and its implications for human disease. *Cell. Mol. Life Sci.* 71: 831–845.
73. Jaitovich, A., M. Angulo, E. Lecuona, L. A. Dada, L. C. Welch, Y. Cheng, G. Gusarova, E. Ceco, C. Liu, M. Shigemura, et al. 2015. High CO_2 levels cause skeletal muscle atrophy via AMP-activated kinase (AMPK), FoxO3a protein, and muscle-specific Ring finger protein 1 (MuRF1). *J. Biol. Chem.* 290: 9183–9194.
74. Myllymäki, H., and M. Rämet. 2013. Transcription factor zfh1 downregulates *Drosophila* Imd pathway. *Dev. Comp. Immunol.* 39: 188–197.
75. Meigh, L., S. A. Greenhalgh, T. L. Rodgers, M. J. Cann, D. I. Roper, and N. Dale. 2013. CO_2 directly modulates connexin 26 by formation of carbamate bridges between subunits. *eLife* 2: e01213.
76. Vilella, A. J., J. Severin, A. Ureta-Vidal, L. Heng, R. Durbin, and E. Birney. 2009. EnsemblCompara GeneTrees: complete, duplication-aware phylogenetic trees in vertebrates. *Genome Res.* 19: 327–335.